A&A 380, 72–80 (2001)
DOI: 10.1051/0004-6361:20011365

Astronomy & Astrophysics

VLBI monitoring of a sample of 15 AGN at 22 GHz

I. Data

K. Wiik[1,2], E. Valtaoja[1,3], and K. Leppänen[4]

[1] Tuorla Observatory, Väisäläntie 20, 21500 Piikkiö, Finland
[2] Metsähovi Radio Observatory, Metsähovintie 114, 02540 Kylmälä, Finland
[3] Department of Physical Sciences, University of Turku, 20100 Turku, Finland
[4] Nokia Research Center, PO Box 407, 00045 Nokia Group, Finland

Received 31 July 2001 / Accepted 25 September 2001

Abstract. We have observed a sample of 15 bright active galactic nuclei (AGN) three times during 1992–1996 using the global 22 GHz VLBI network. The sample consists of all sources in the complete 2 Jy catalog of Valtaoja et al. that were not observed at 22 GHz VLBI before the first epoch. We will present submilliarcsecond resolution VLBI images of these sources with description of the observations and data analysis techniques. Part II of this paper will contain a detailed analysis of the images.

Key words. galaxies: jets – galaxies: active

1. Introduction

VLBI observations with highest possible resolution are necessary for investigating the physics of shocked relativistic jets in the cores of active galaxies. Typical variability timescales for 22/37 GHz total flux density flares are of the order of 0.5 years (Valtaoja & Teräsranta 1994). Even in relatively nearby superluminal quasars, the shocks are already several years old and therefore in their final decay stages by the time they can be resolved from the core with standard VLBI at lower frequencies. In fact most of the strong millimeter flares in blazars appear only as "core brightenings" in VLBI maps (Valtaoja et al. 1999; Savolainen et al. 2001). Sub-mas or even μas resolution is required to follow the structural evolution of the growing shocks. Such data can even be used for cosmological purposes (Wiik & Valtaoja 2001).

A drawback with the available high-frequency VLBI data is that it is heavily concentrated on just a few well known favorite objects such as 3C 279 (e.g. Wehrle et al. 2001). Until recently (Lister 2001a; Lister 2001b, this work) we have lacked data on complete samples of even the brightest sources, and may therefore have a rather biased view on the VLBI properties of various classes of AGN.

Our aims were to obtain high-frequency and high resolution VLBI data on a representative sample of AGN. In this paper we describe the observations and present three-epoch 22 GHz global VLBI images of 15 AGN observed during 1992–1996. A follow-up paper will include a full discussion of the individual sources as well as comparisons with Metsähovi total flux density monitoring data (Teräsranta et al. 1998).

Send offprint requests to: Kaj Wiik, e-mail: kaj.wiik@iki.fi

2. The sample

Our sample is based on the complete Northern hemisphere sample of compact AGN (Valtaoja et al. 1992) The selection is based on the high-frequency characteristics of AGN, with the selection criteria $S_{22\ \mathrm{GHz}} > 2$ Jy and $\alpha_{2.7-5\ \mathrm{GHz}} > -0.5$. The 47 sources fulfilling these criteria are bright and likely very compact.

The extremely long baselines in future high-frequency (>22 GHz) space VLBI set stringent requirements to the brightness temperature (T_b) and consequently the compactness of the source. The observation will use the UV-plane optimally only if there is still detectable correlated flux at the longest baselines. For this reason, the sources of our sample would be prime candidates for future high-frequency space-VLBI observations.

It would not have been feasible to observe all of these sources, so an additional criterion was used. Up to 1992 15 of these 47 sources had not been observed with 22 GHz VLBI and thus these formed our final sample. The sample is representative since it includes all the main classes of AGN: 3 highly polarized quasars (HPQ), 5 low polarization quasars (LPQ), 6 BL Lac objects (BLO) and one radio galaxy (RG). In addition, several of these sources have been classified as GPS/CSS/CSO sources or

Table 1. Sources.

Source	Aliases	Class	z	reference for z
0106+013	OC 012	HPQ	2.0989	(Hewett et al. 1995)
0202+149	4C 15.05, NRAO 91	HPQ	0.405	(Perlman et al. 1998)
0528+134	OG 147	LPQ	2.07	(Hunter et al. 1993)
0754+100	OI 090.4	BLO	0.27/0.66?	(Falomo & Ulrich 2000)
0953+254	OK 290	LPQ	0.709	(White et al. 2000)
1219+285	ON 231	BLO	0.102	(Marcha et al. 1996)
1413+135	OQ 122	BLO	0.247	(Wiklind & Combes 1997)
1418+546	OQ 530	BLO	0.151	(Marcha et al. 1996)
1749+096	OT 081	BLO	0.322	(Hewitt & Burbidge 1989)
1807+698	3C 371, NRAO 548	BLO	0.0511	(de Ruiter et al. 1998)
2021+614	4C 31.56, OW 637	GAL	0.227	(Hewitt & Burbidge 1991)
2134+004	OX 057	LPQ	1.932	(Osmer et al. 1994)
2145+067	OX 076	LPQ	0.999	(Drinkwater et al. 1997)
2201+315	4C 31.63	LPQ	0.295	(Marziani et al. 1996)
2230+114	CTA 102	HPQ	1.037	(Aldcroft et al. 1994)

Table 2. Observations.

Project code	Time (hours)	Bandwidth (MHz)	Telescopes
GL10	48	1.8	15
GL13	24	14	17
GW14	24	14	16

candidates: 0528+134, 0754+100, 1418+546, 2021+614, 2134+004 and 2230+114 (Snellen et al. 1995; Stanghellini et al. 1998; O'Dea et al. 1998; Tornikoski et al. 2001).

3. VLBI observations

The observations took place in November 1992 (GL10), September 1993 (GL13), and October 1996 (GW14) using the global VLBI array composing of 10 Very Long Baseline Array (VLBA) and 6 European VLBI Network (EVN) telescopes: Brewster (Br), Fort Davis (Fd), Hancock (Hn), Kitt Peak (Kp), Los Alamos (La), Mauna Kea (Mk), North Liberty (Nl), Ovens Valley (Ov), Pie Town (Pt), Saint Croix (Sc) and Effelsberg (Ef), Jodrell Bank (Jb), Medicina (Mc), Metsähovi (Mh), Noto (Nt), Onsala (On) respectively and Green Bank (Gb) and VLA(Y) (1 telescope) of National Radio Astronomy Observatory (NRAO).

Unfortunately all telescopes were not available for every epoch due to technical problems or had to be flagged out because of bad weather. 15[1], 17[2] and 16[3] telescopes produced useful data in experiments GL10, GL13 and GW14 respectively. Further details are presented in Table 2.

To keep both the thermal and especially the imaging noise level as low as possible, it was important to have at least 2×12 hours of observing time available. A full 48-hour run gives two possibilities to observe a given point in the UV-plane, thus reducing the effects of bad weather and giving a better possibility for a good UV-coverage. This compensates well the sensitivity limitations of narrow Mk II bandwidth. Although the first epoch was recorded using the old MK II system to video cassettes, performance was nearly equal to the second epoch which was hampered by poor weather.

As can be seen from the two examples Fig. 1, the individual scans were kept short and the sources were observed as regularly as possible to obtain an even UV-coverage but still trying to maintain acceptable overall observing efficiency. To improve efficiency further, the slowest telescope had to be commanded to step over sources occasionally, in milder cases the recorders were started although the slowest telescope was still slewing.

Furthermore, it was necessary to split the global array to two (EU and US) subarrays during some periods to improve observing efficiency. This caused serious problems during data reduction, because AIPS did not support subarraying at the time. On the other hand, without subarraying, e.g. the Mauna Kea telescope would have been observing only small fraction of the time. The scans that were recorded with the two subarrays had to be extracted and retagged to the correct source manually. Currently AIPS supports subarraying through the task USUBA.

4. Data reduction

For the most part standard procedures were used in calibration and mapping, exceptions are outlined below. The correlated visibilities were read to AIPS where a priori amplitude calibration was applied and fringe fitting and preliminary data editing was performed.

Further processing was carried out using Difmap (Shepherd 1997). The visibilities of clearly point-like simple sources were calibrated by using a model which was first consisting only one or two circular Gaussian components. After convergence, phase self-calibration was

[1] Eb, Mc, Mh, No, On, Gb, Br, Hn, Kp, La, Nl, Ov, Pt.

[2] Eb, Mc, Mh, No, On, Gb, Y, Br, Fd, Hn, Kp, La, Mk, Nl, Ov, Pt, Sc.

[3] Eb, Mh, No, On, Gb, Y, Br, Fd, Hn, Kp, La, Mk, Nl, Ov, Pt, Sc.

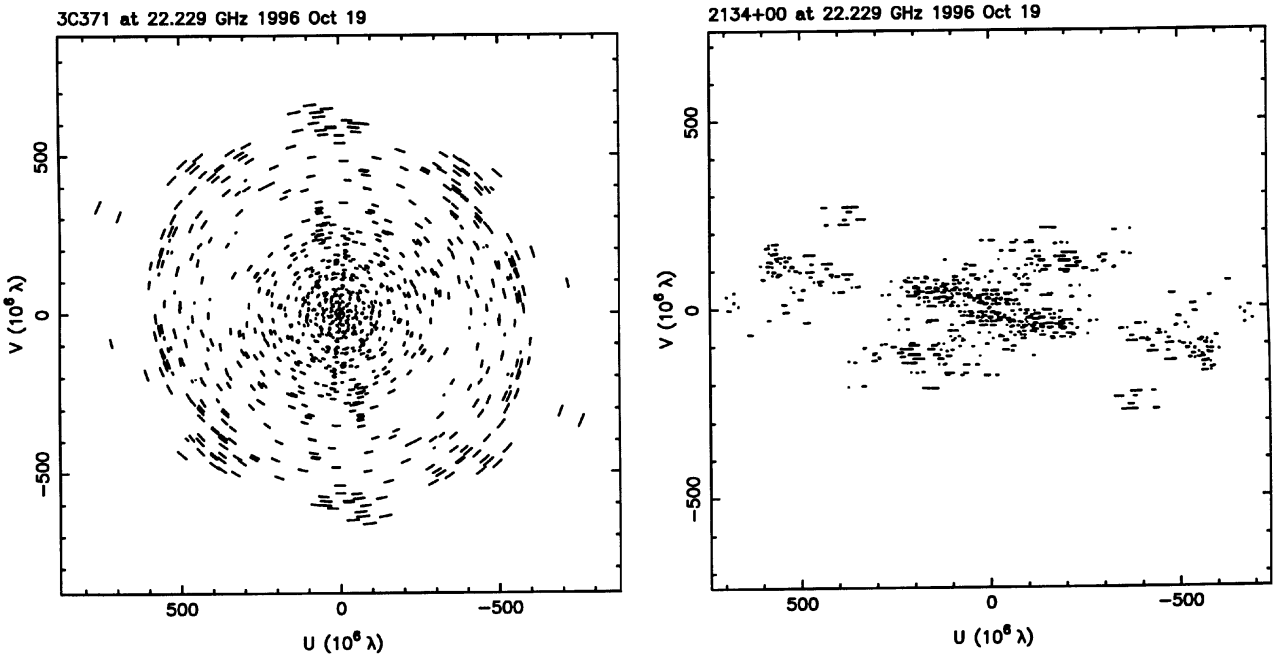

Fig. 1. UV-coverages for the highest (1807+698) and lowest (2134+004) declination sources.

performed and the procedure was repeated until a reasonable fit was obtained *to the closure phases*. Then, if necessary, more model components were added to the model. For more diffuse, extended sources, e.g. smooth jets, CLEAN algorithm was used instead of modelfit.

If the model flux reached that of the data and there was a good fit to the closure phases but with clear residuals in visibility amplitudes, amplitude self-calibration was performed cautiously using as long solution intervals as possible. If rapidly varying amplitude errors occurred only in the visibilities of a single telescope, the complex gains of the remaining telescopes were set to a fixed value and full self calibration was performed with appropriate solution interval. This technique permits to use relatively short solution intervals safely without a significant effect to the total flux.

In some cases the Difmap modelfit or CLEAN algorithm seemed to converge well, but resulted noticeable residuals in closure phases. Occasionally tweaking the starting model helped to climb from this local minimum but usually the data had to be either re-edited or self-calibrated in amplitude. If the amplitude selfcalibration was successful, a convergence was achieved both in visibility phases and amplitudes and also in closure phases. However, if amplitude selfcalibration was used carelessly, it resulted a map with lowered total flux, poor fit of the model to the closure phases and significantly lower dynamic range.

Nearly all of the a priori amplitude calibration information of the EVN MKIIIa stations was lost from the third epoch observations because of a bug in the procedures that were sent to the telescopes. A difference in the syntax between MKIIIa and VLBA terminals caused the system noise temperature ($T_{\rm sys}$) measurement procedure to fail and only sparse uncalibrated total power readings were recorded.

To salvage at least some information from the long intercontinental baselines, a well calibrated map was first done using only VLBA data. The complex gains of the VLBA antennas were then set to a fixed value and the low-resolution map was used as a starting model to calibrate the gains of the EVN antennas. The closure phases gave vital information about whether the amplitude calibration and the model image were converging. Often a dead end was reached and the whole procedure had to be restarted using a slightly different starting model. In most cases the results were satisfactory and the dynamic range was comparable to the second epoch.

During the reduction of the third epoch, it was found that some the sources were more extended than were anticipated at the beginning of this project. The VLBA 15 GHz survey (Kellermann et al. 1994) was used to check of any weak components outside the imaging area of the first and second epoch, and the first two epochs were reprocessed when necessary.

The first epoch was rereduced using faster computers and using information from the later epochs. This increased the dynamic range on average by a factor of two and in some cases significant artifacts were detected and eliminated.

5. VLBI maps

The maps were plotted semiautomatically with a Perl Data Language (PDL, `http://pdl.perl.org`) program using the Difmap image-plane FITS files. The off-source root mean square (rms) noise level was determined by

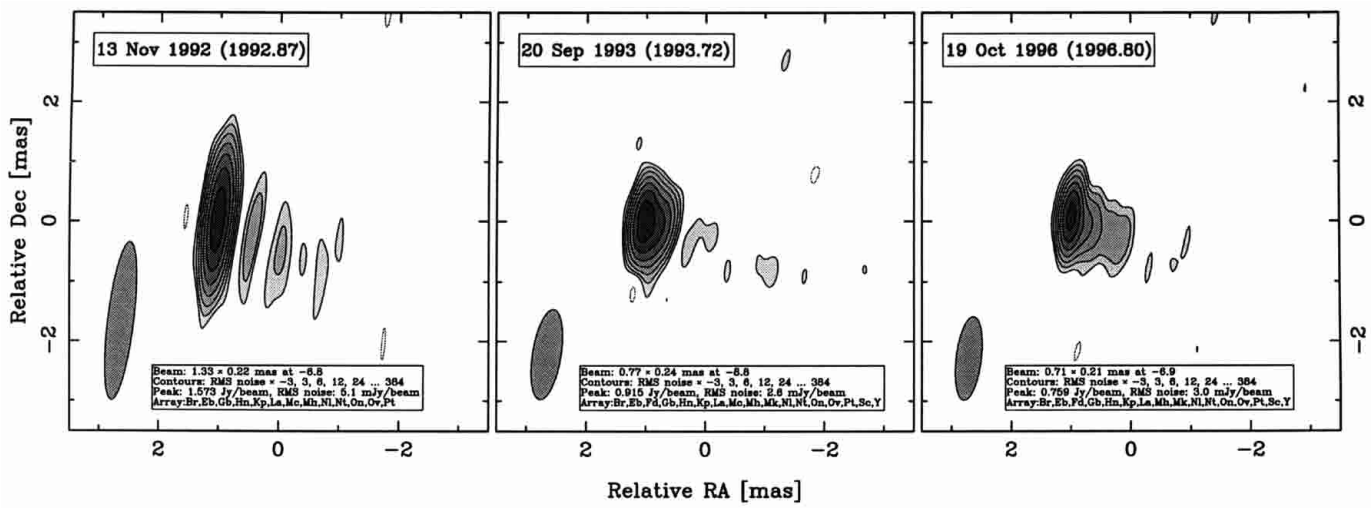

Fig. 2. 0106+013 (OC 012). The contour levels in the following maps start from ±two times below of the root mean square (rms) noise level and the following flux levels increase in powers of two. Those stations that have contributed more than 0.1% of the total number of visibilities are included in the array list. Please note that the greyscale levels vary from epoch to epoch.

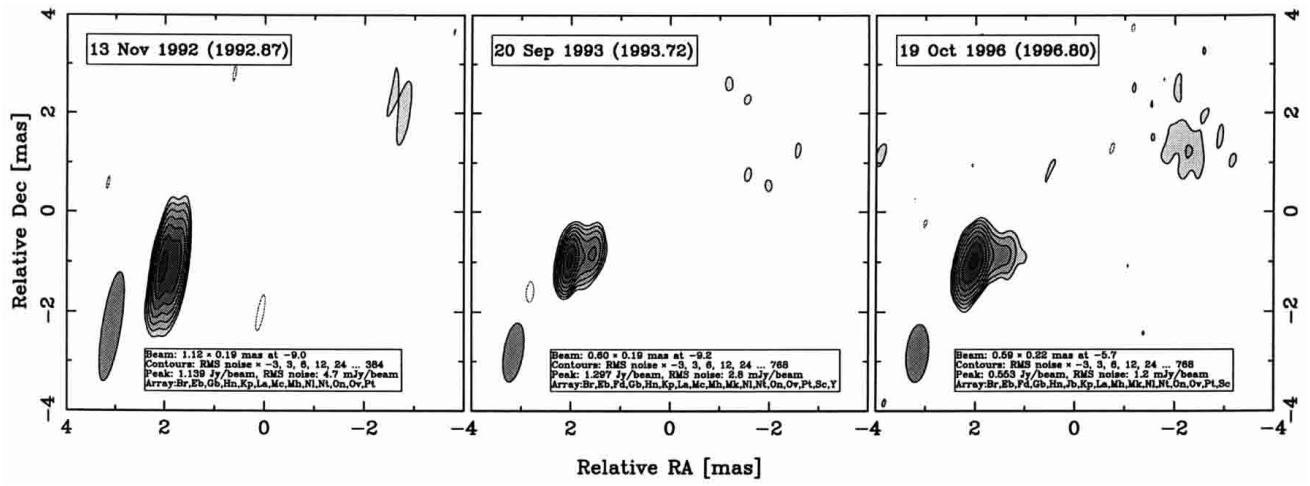

Fig. 3. 0202+149 (4C 15.05, NRAO 91).

fitting a Gaussian to the histogram of all of the binned image data around the zero-level. This noise level estimate is conservative because some low-level source emission is taken as noise. However, because most of the flux in the sources is contained in small components, this does not cause noticeable problems as can be seen from the maps.

The final maps are presented in Figs. 2–16. The first two contours represent ±three times the rms noise level and the following flux levels are increasing in factors of two. Uniform weighting has been used and the restoring beam is calculated from the uv-coverage for each epoch separately.

This survey revealed a rich variety of morphologies and behaviors from the most compact and static to very extended and variable both in flux and morphology. A detailed analysis of each source will be presented in part II of this paper.

6. Conclusions

We have presented three-epoch 22 GHz global VLBI images of 15 sources. For two sources (0106+013 and 0754+100) no previous VLBI maps at 22 GHz or higher frequencies have been published.

Our observations reveal a wide variety of morphologies within the innermost few parsecs of the sources. In part II of this paper we will discuss the morphologies and comparisons with total flux density monitoring data in detail. VLBI observations of complete samples with both high resolution and high dynamic range are needed to elucidate how the parsec-scale structure relates to other properties such as the gamma-ray luminosity.

Acknowledgements. We gratefully acknowledge R. Schilizzi for help in the first stages of this project and K. Kellermann for giving permission to use the VLBA 15 GHz survey data. The European VLBI Network is a joint facility of European and Chinese radio astronomy institutes funded by their national

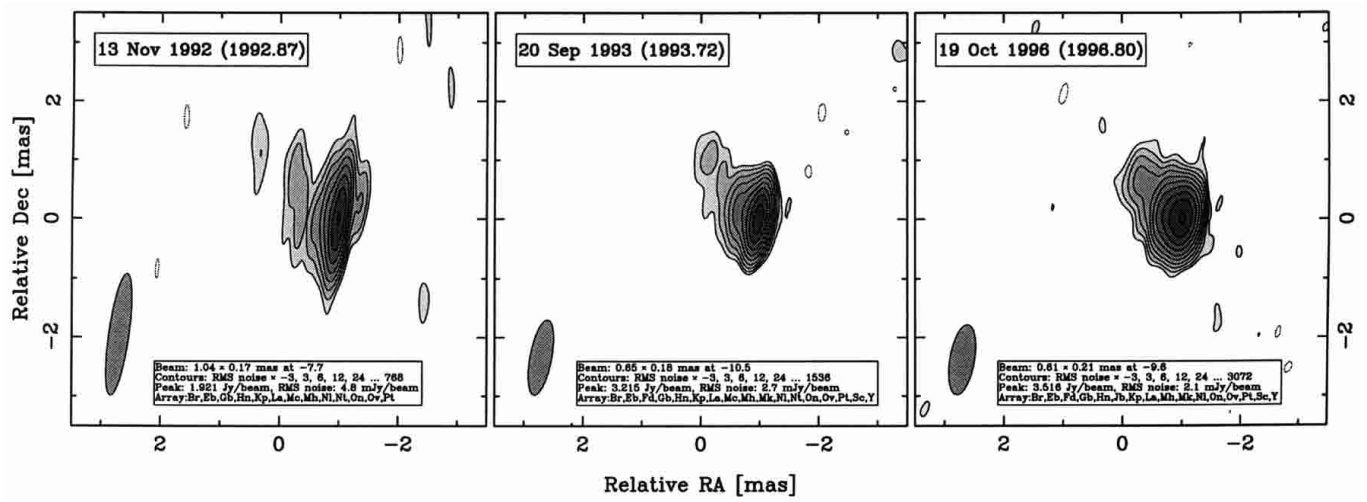

Fig. 4. 0528+134.

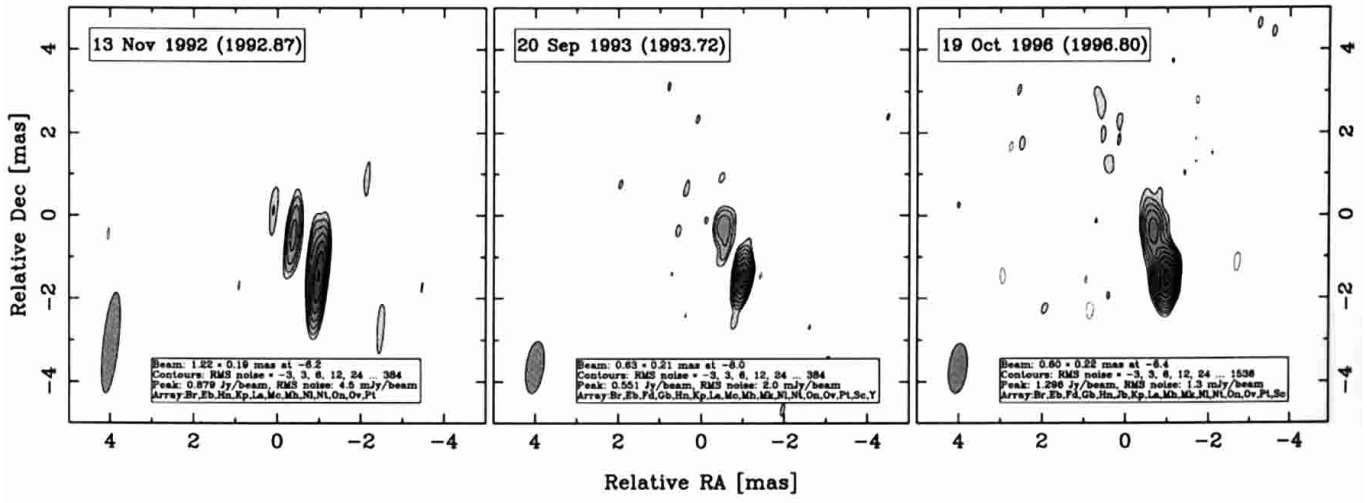

Fig. 5. 0754+100 (OI 090.4).

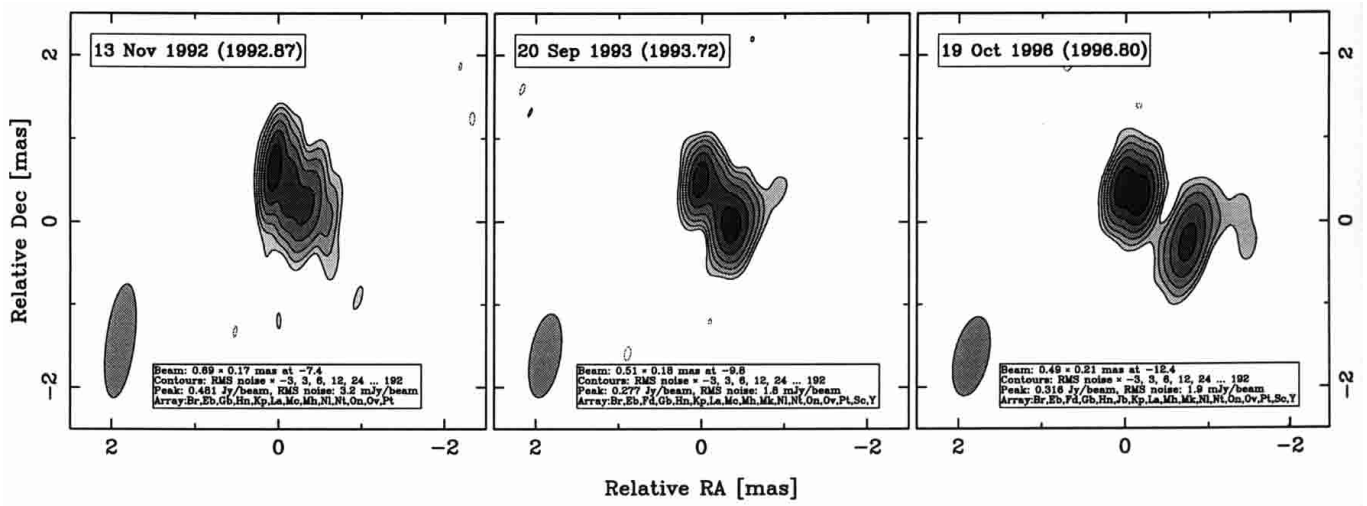

Fig. 6. 0953+254 (OK 290).

research councils. The National Radio Astronomy Observatory is a facility of the National Science Foundation operated under cooperative agreement by Associated Universities, Inc. This research has been partly funded by grants from the Academy of Finland. K.W. acknowledges grants from Emil Aaltonen Foundation and Vilho, Yrjö and Kalle Väisälä Foundation for this work.

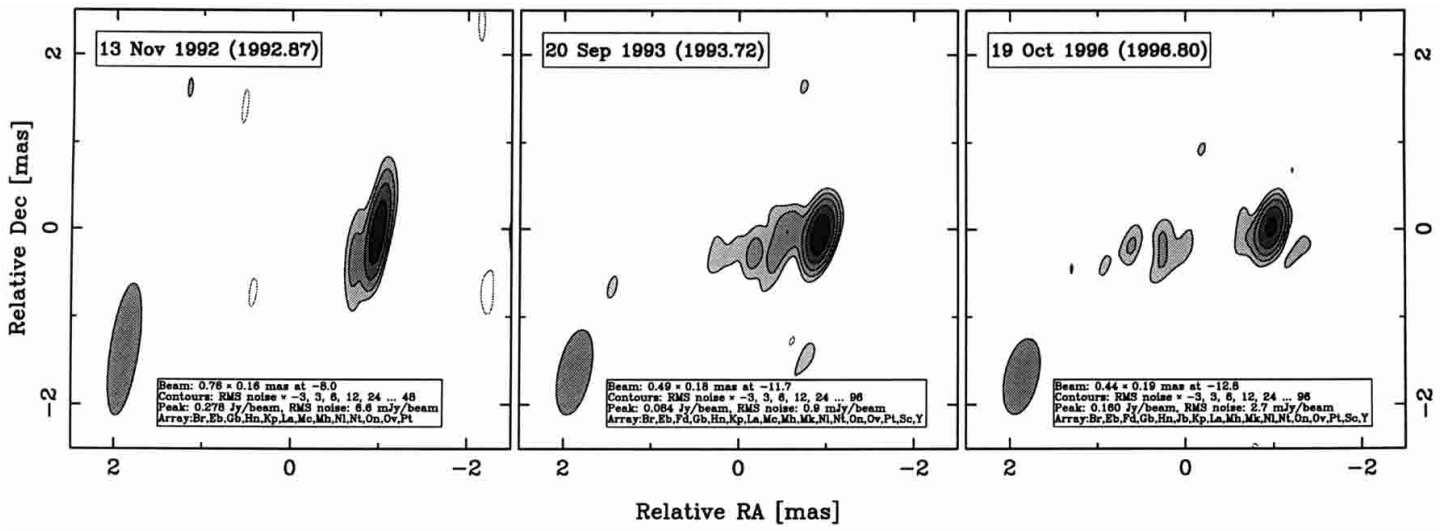

Fig. 7. 1219+285 (ON 231).

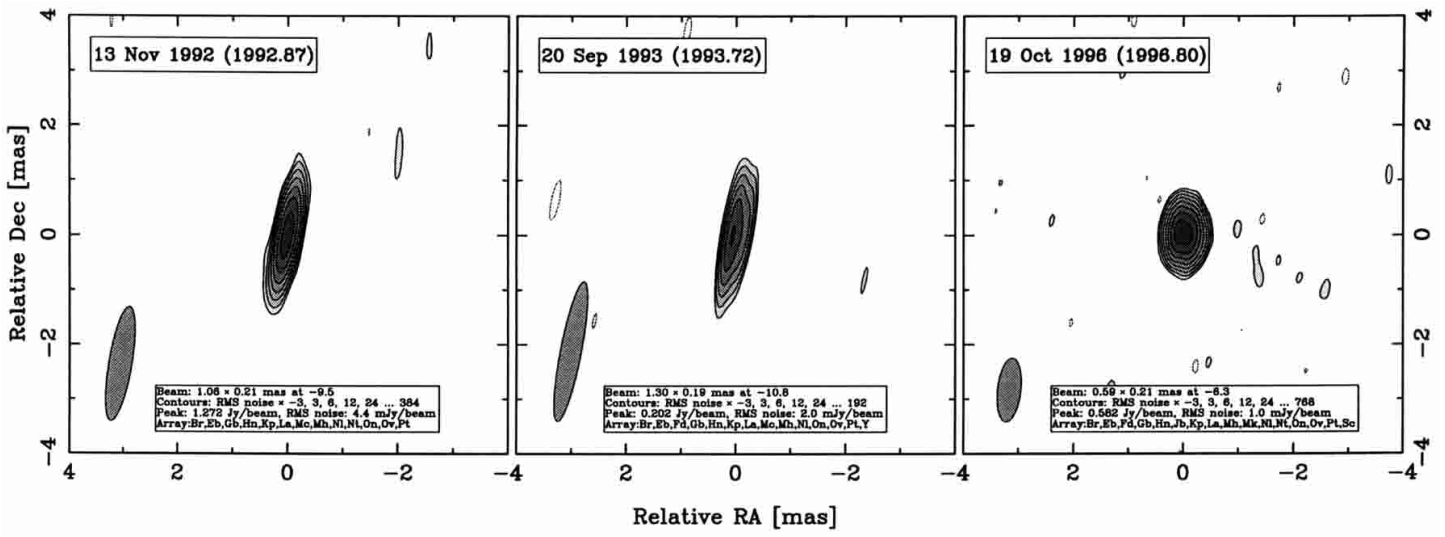

Fig. 8. 1413+135.

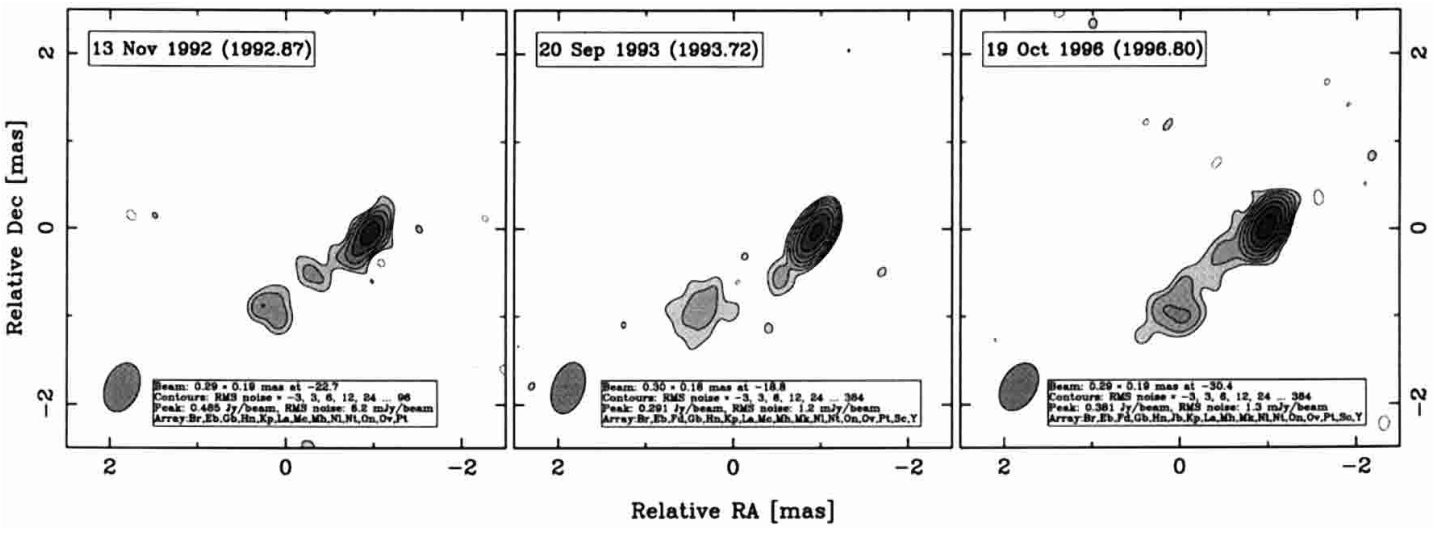

Fig. 9. 1418+546 (OQ 530).

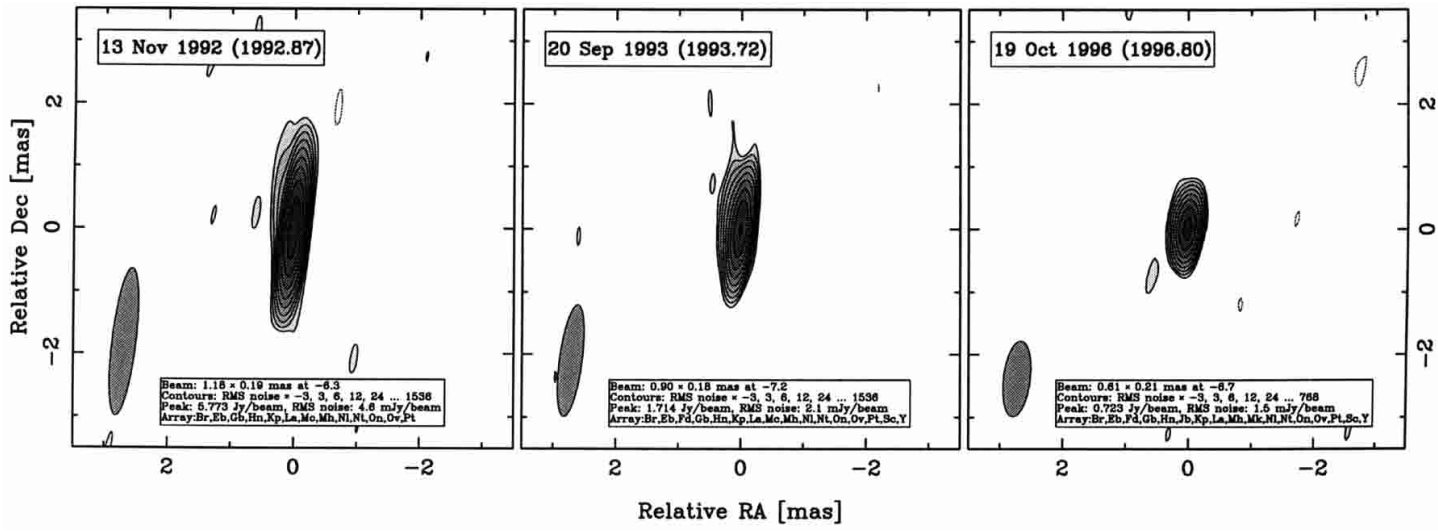

Fig. 10. 1749+096 (OT 081).

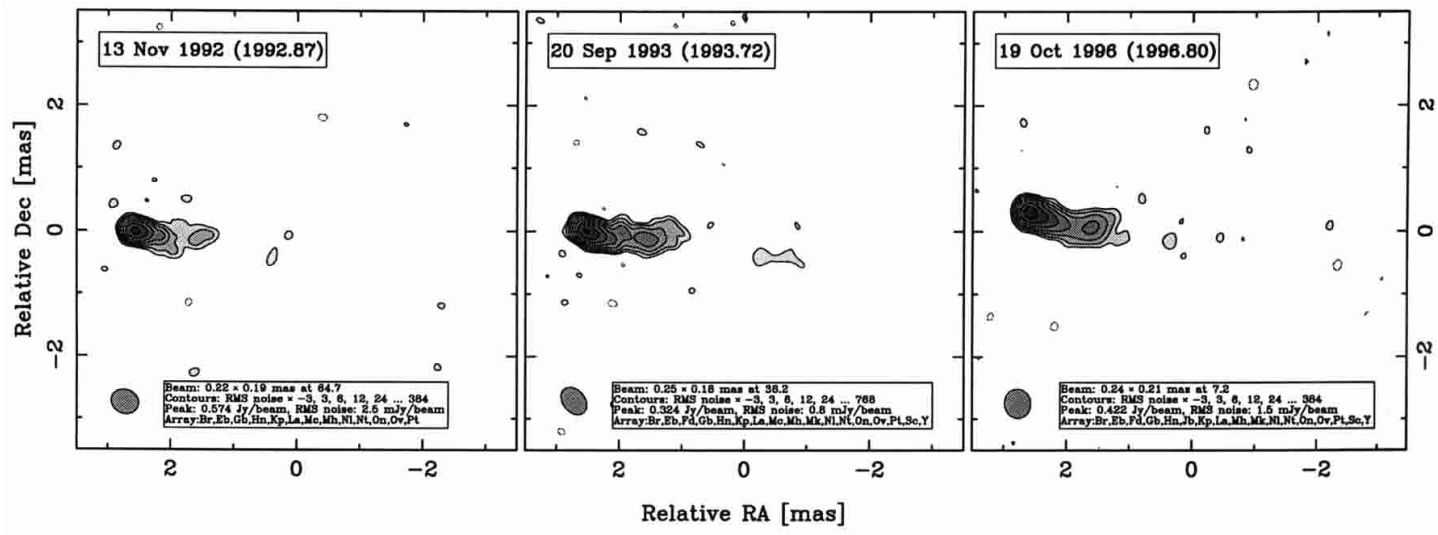

Fig. 11. 1807+698 (3C 371).

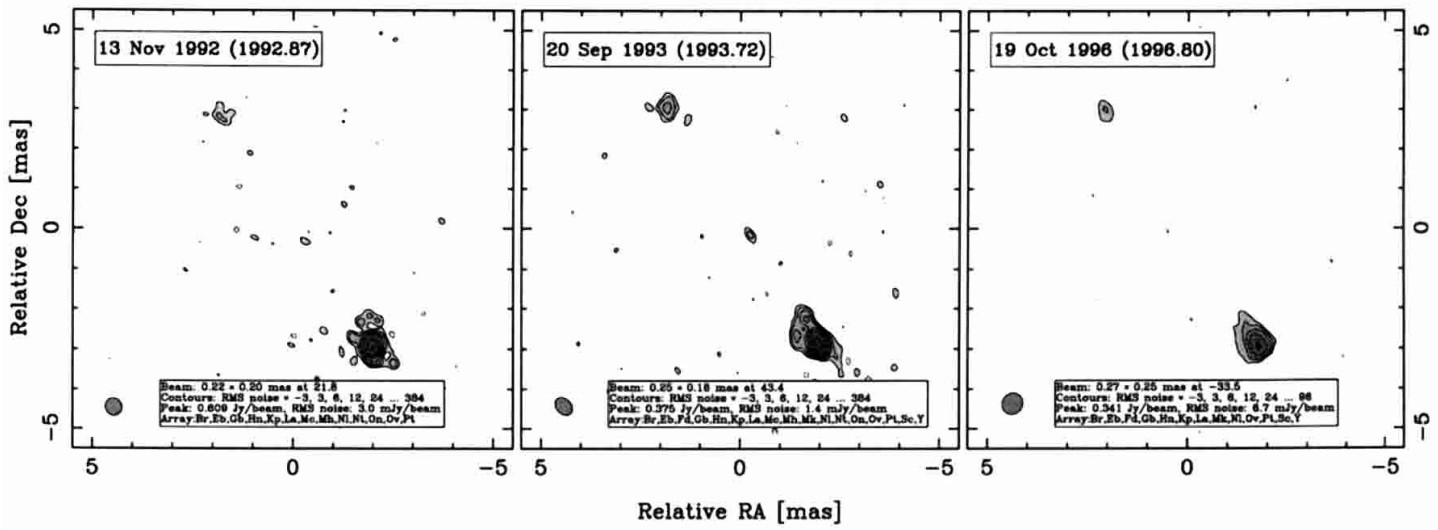

Fig. 12. 2021+614 (4C 31.56, OW 637).

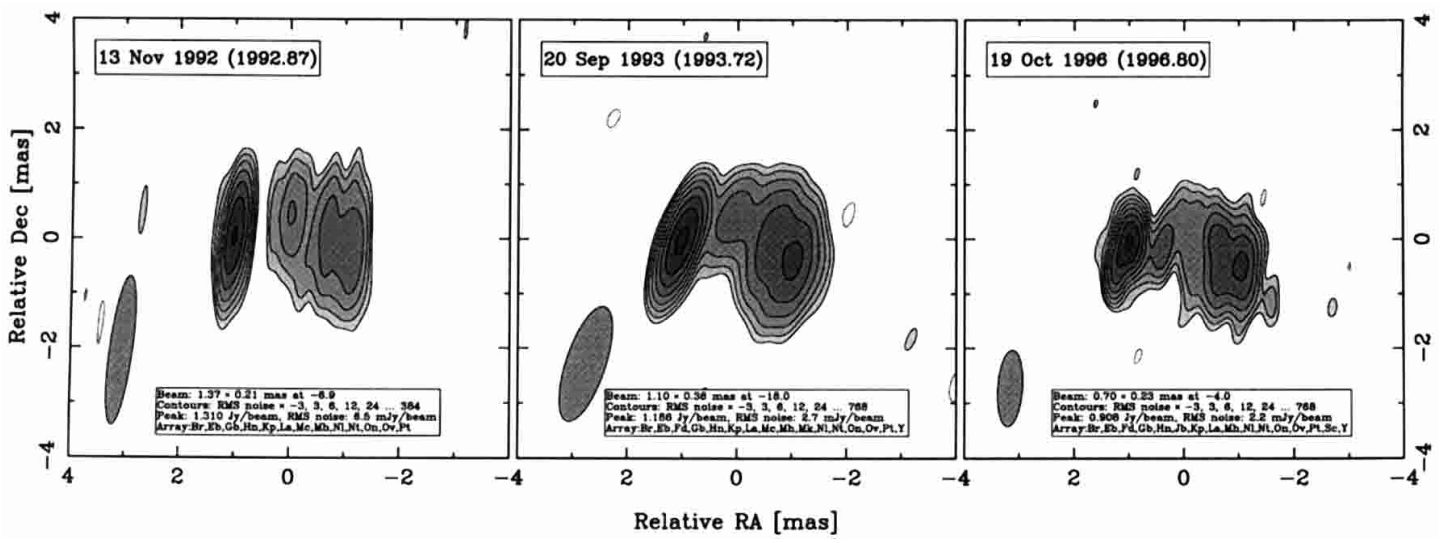

Fig. 13. 2134+004 (OX 057).

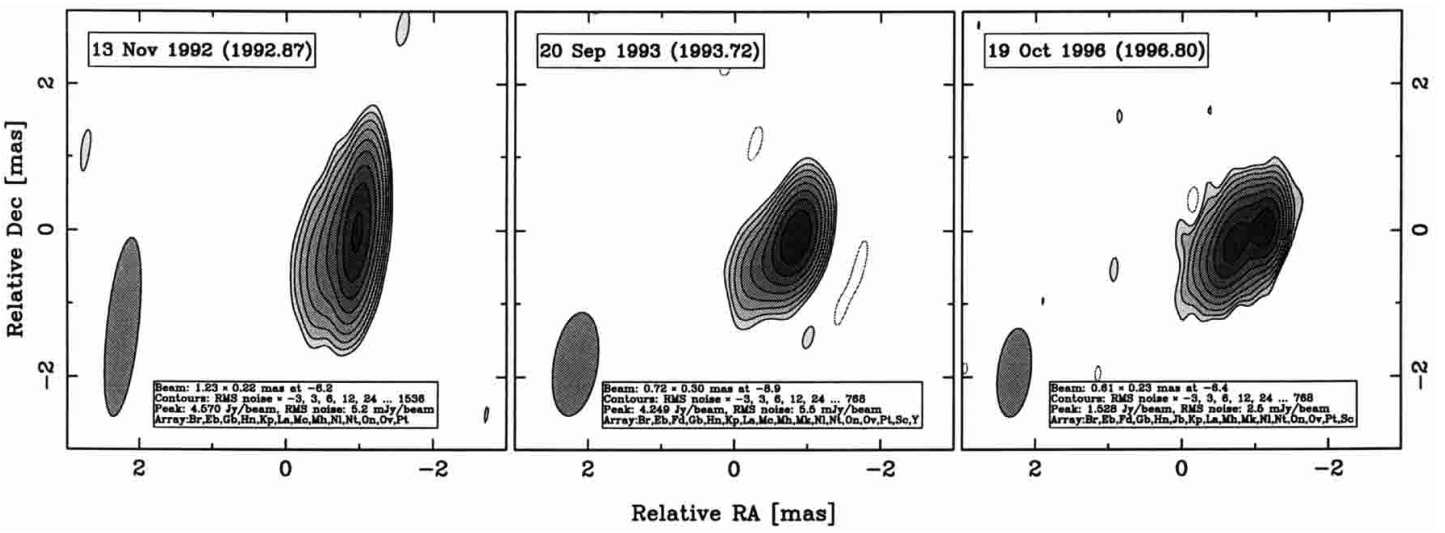

Fig. 14. 2145+067.

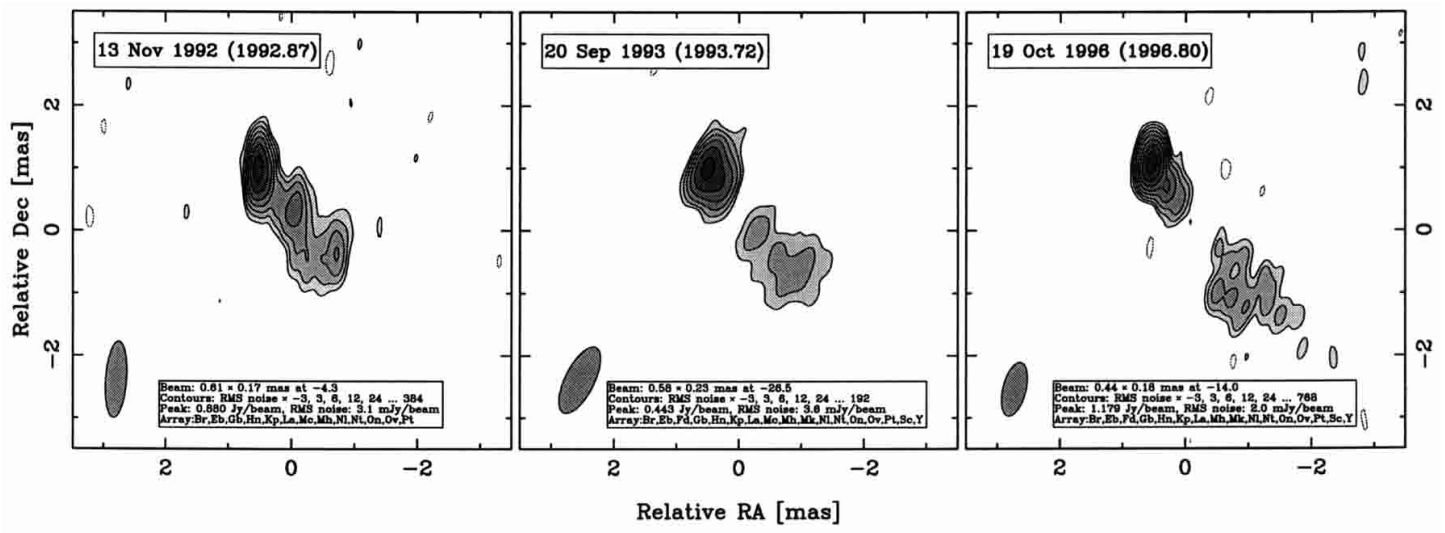

Fig. 15. 2201+315 (4C 31.63).

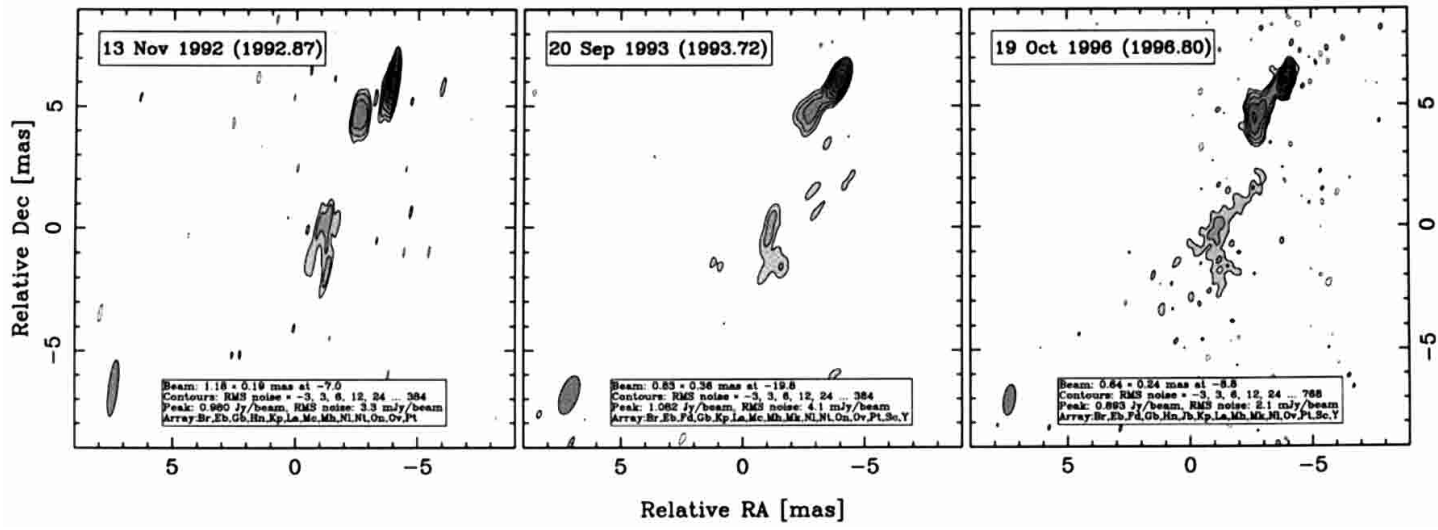

Fig. 16. 2230+114 (CTA 102).

References

Aldcroft, T. L., Bechtold, J., & Elvis, M. 1994, ApJS, 93, 1

de Ruiter, H. R., Parma, P., Stirpe, G. M., et al. 1998, A&A, 339, 34

Drinkwater, M. J., Webster, R. L., Francis, P. J., et al. 1997, MNRAS, 284, 85

Falomo, R., & Ulrich, M. 2000, A&A, 357, 91

Hewett, P. C., Foltz, C. B., & Chaffee, F. H. 1995, AJ, 109, 1498

Hewitt, A., & Burbidge, G. 1989, ApJS, 69, 1

Hewitt, A., & Burbidge, G. 1991, ApJS, 75, 297

Hunter, S. D., Bertsch, D. L., Dingus, B. L., et al. 1993, ApJ, 409, 134

Kellermann, K. I., Zensus, J. A., Vermuelen, R. C., & Cohen, M. H., 15 GHz VLBA Survey
`http://www.cv.nrao.edu/2cmsurvey/`

Lister, M. L. 2001, ApJ, accepted

Lister, M. L., Tingay, S. J., & Preston, R. A. 2001, ApJ, 554, 948

Marcha, M. J. M., Browne, I. W. A., Impey, C. D., et al. 1996, MNRAS, 281, 425

Marziani, P., Sulentic, J. W., Dultzin-Hacyan, D., et al., ApJS, 104, 37

O'Dea, C. P. 1998, PASP, 110, 493

Osmer, P. S., Porter, A. C., & Green, R. F. 1994, ApJ, 436, 678

Perlman, E. S., Padovani, P., Giommi, P., et al. 1998, AJ, 115, 1253

Savolainen, T., Valtaoja, E., Wiik, K., Jorstad, S. G., & Marscher, A. P. 2001, A&A, in preparation

Shepherd, M. C. 1997, Astronomical Data Analysis Software and Systems VI, ASP Conf. Ser., 125, 6, 77

Snellen, I. A. G., Zhang, M., Schilizzi, R. T., et al. 1995, A&A, 300, 359

Stanghellini, C., O'Dea, C. P., Dallacasa, D., et al. 1998, A&AS, 131, 303

Teräsranta, H., Tornikoski, M., Mujunen, A., et al. 1998, A&AS, 132, 305

Tornikoski, M., Jussila, I., Johansson, P., Lainela, M., & Valtaoja, E. 2001, AJ, 121, 1306

Tschager, W., Schilizzi, R. T., Röttgering, H. J. A., et al. 2000, A&A, 360, 887

Valtaoja, E., Lähteenmäki, A., & Teräsranta, H. 1992, A&AS, 95, 73

Valtaoja, E., & Teräsranta, H. 1994, A&A, 289, 35

Valtaoja, E., Lähteenmäki, A., Teräsranta, H., et al., ApJS, 120, 95

White, R. L., Becker, R. H., Gregg, M. D., et al. 2000, ApJS, 126, 133

Wehrle, A. E., Piner, B. G., Unwin, S. C., et al. 2001, ApJS, 133, 297

Wiik, K., & Valtaoja, E. 2001, A&A, 366, 1061

Wiklind, T., & Combes, F. 1997, A&A, 328, 48